Using $^{210}Pb_{ex}$ measurements to quantify soil redistribution along two complex toposequences in Mediterranean agroecosystems, northern Spain

Gaspar, L.[1, 2*], Navas, A.[2], Machín, J.[2], Walling, D.E.[3]

[1] Cranfield University, Cranfield Water Sciences Institute, Cranfield, Bedfordshire MK43 0AL, United Kingdom.

[2] Department of Soil and Water, Estación Experimental de Aula Dei, EEAD-CSIC. Avda Montañana 1005, 50059 Zaragoza, Spain.

[3] Department of Geography, College of Life and Environmental Sciences, University of Exeter. Amory Building, Rennes Drive, Exeter EX4 4RJ, United Kingdom.

*Corresponding author. E-mail, leticia.gaspar.ferrer@gmail.com, l.gasparferrer@cranfield.ac.uk,

Abstract

Information on soil redistribution rates associated with the intricate patterns of Mediterranean agroecosystems is a key requirement for assessing both soil degradation, and off-site sediment problems that can affect downstream water bodies. Excess lead-210 ($^{210}Pb_{ex}$) measurements provide a very effective means of documenting spatial patterns of rates of soil redistribution in different landscapes, but to date the approach has not been widely used in mountain Mediterranean landscapes. This research aims to use $^{210}Pb_{ex}$ measurements to estimate soil redistribution rates on slopes uncultivated and under cultivation, within two complex toposequences located in the vicinity of Estaña Lake, characterized by an intricate mosaic of land use, steep slopes and anthropogenic modification (e.g. terraces and tracks), which are typical of these agroecosystems in northeastern Spain. A perceptual model is developed to account for the soil redistribution dynamics along both toposequences. This provides a simple and novel methodology adapted to Mediterranean agroecosystems, which besides using information on soil redistribution rates provided by $^{210}Pb_{ex}$ measurements, also takes into account variations in land use and the presence of linear landscape elements, which modify runoff and soil redistribution processes and sediment connectivity along the toposequences. The results show that erosion predominated on the steep cultivated slopes, but lower soil redistribution rates were found on the uncultivated slopes. On the flat areas at the bottom of both transects, deposition was dominant. Variations in land use and the presence of linear landscape elements control soil redistribution processes. Such elements can perform the role of Ecological Focus Areas (EFAs), proposed within 'The Green' Common Agricultural Policy for 2014, in which at least 7 % of a farmer's land should comprise EFAs, which can include terraces, landscape features, buffer strips and afforested areas.

Keywords: $^{210}Pb_{ex}$; Soil erosion; Soil redistribution rates; land use; CAP; linear landscape elements; Mediterranean agroecosystems.

1 Introduction

Soil degradation by water erosion represents one of the major environmental problems facing the sustainable management of soil and soil productivity. Cultivation is seen as a key factor promoting soil mobilization and soil loss. Other related effects, including the mobilization and transport of sediment-associated contaminants (pesticides, fertilizers) and the siltation of wetland areas must also be taken into account to protect fragile agroecosystems. In addition, soil erosion transfers soil organic carbon from topsoil to deposition sinks in the landscape and promotes soil carbon replacement at eroded sites (Ritchie and McCarty, 2003).

Increased awareness of the problems of soil loss in the last decade has promoted actions to conserve soil under the European Common Agricultural Policy (CAP), including the most recent Green Areas initiative. In Mediterranean mountain agroecosystems large areas of agricultural land were abandoned during the past century as a result of major socio-economic changes. In recent years, however, some steep marginal lands have been returned to cultivation under the European Agrarian Policy (García-Ruiz et al., 2008; García-Ruiz, 2010; Gaspar et al., 2013). The study area selected for this research is a good example of mountain areas in northern Spain, which illustrates many of the problems associated with steep slopes, high rainfall intensity, changes of land use, and especially the abandonment of the less productive land located on steep slopes. Previous studies highlight the importance of soil erosion in the study area, especially in cultivated areas. For cropland areas, Navas et al. (2012a) used caesium-137 (^{137}Cs) measurements to estimate erosion rates as high as 108 Mg ha^{-1} year^{-1}, while López-Vicente and Navas (2010) predicted severe erosion rates (> 100 Mg ha^{-1} year^{-1}), using a combination of the RMMD and SED models, in gullies on Keuper facies. In the study area, the term 'uncultivated' has been used to refer to a range of conditions including areas of undisturbed natural vegetation and areas under Mediterranean forest and scrub, as well as old abandoned fields in long-term fallow (> 100 years), which are now covered by dense scrub, and the more recently abandoned fields (ca. 50 years) that have a much reduced vegetation cover. This leads to the development of a spatial pattern of vegetated patches and bare cultivated inter-patch areas, affecting water redistribution and it is well established that vegetation development and vegetation structure affect the connectivity of runoff and soil redistribution processes on slopes (Cerdá 1997).

Lead-210 (^{210}Pb) is a natural geogenic radioisotope (half life, 22.2 yr) of the uranium decay series. Decay of radium-226 in the soil and regolith releases radon-222 (^{222}Rn), which in turn decays to ^{210}Pb. Some of the ^{222}Rn diffuses upward through the soil and enters the atmosphere where it decays to ^{210}Pb and is returned to the earth's surface as fallout. Fallout ^{210}Pb reaching the soil surface is rapidly adsorbed by clay minerals and organic matter, and its subsequent redistribution is controlled by soil redistribution processes in a manner similar to ^{137}Cs (Walling and He, 1999a, b). This fallout ^{210}Pb is termed unsupported or excess ^{210}Pb ($^{210}Pb_{ex}$), since it is not in equilibrium with its parent ^{226}Ra. $^{210}Pb_{ex}$, like ^{137}Cs, offers the potential for use as a tracer in estimating rates of soil redistribution. However, $^{210}Pb_{ex}$ measurements have been less widely used for estimating soil redistribution rates than ^{137}Cs, although their use has increased significantly in recent years (e.g. Wallbrink and Murray, 1993; Walling and Quine, 1995; He, Q. and Walling, D.E. 1996; Zhang, et al., 2006; Kato et al., 2010; Porto and Walling, 2012; Benmansour et al., 2013).

The continuous input of $^{210}Pb_{ex}$ fallout through time means that the contemporary $^{210}Pb_{ex}$ inventory in the soil will reflect soil redistribution and thus loss and gain of $^{210}Pb_{ex}$ occurring within a period equivalent to four times the half-life, and thus the past 100 years (Walling et al., 2003). However, the effect of past changes in the $^{210}Pb_{ex}$ inventory, caused by erosion and deposition, on the contemporary inventory, will progressively decline as the period of time elapsed increases and this must be taken into account when interpreting the impact of the erosional history of a study site on the magnitude of the contemporary $^{210}Pb_{ex}$ inventory. This inventory will clearly be more sensitive to recent soil redistribution, and the estimate of the mean rate of soil redistribution for the past ca. 100 years provided by the conversion model used to estimate the soil redistribution rate from a comparison of the inventory measured at a sampling point with the local reference inventory is likely to be biased towards the recent erosional history of the study site.

In order to understand soil redistribution dynamics in the intricate toposequences that are characteristic of the typical agroecosystems of northern Spain, it is important to know how the interfacing of patches of different land use and linear landscape elements modify soil redistribution processes and the sediment connectivity along the slopes. The use of $^{210}Pb_{ex}$ measurements provides a means of investigating such systems. Their use to investigate both cultivated and uncultivated soils and to quantify sediment sources and sinks along slopes of different aspect represents a novel application, particularly within a mountain agricultural area. The use of $^{210}Pb_{ex}$ measurements to document soil redistribution rates and analysis of the factors that affect soil redistribution along toposequences of different aspect affords a means of developing an improved understanding of the role of land use, soil type and slope gradient in Mediterranean agroecosystems. Additionally, the development of a perceptual model of soil movement of redistribution rates, which take into account changes in land uses and the presence of linear landscape elements, is seen as potentially offering a new tool to elucidate sediment connectivity in intricate landscapes. This is of importance for developing ‘green’ agricultural practices, as 'The Green' CAP proposes that at least 7 % of farmland should be converted to Ecological Focus Areas.

The objectives of this study were therefore to use $^{210}Pb_{ex}$ measurements to estimate the long-term mean annual rate of soil redistribution on cultivated and uncultivated soils along two slope transects representatives of Mediterranean agroecosystems in NE of Spain. Its results aim to contribute to a better understanding of the impact of land use and the presence of linear landscape elements (both natural features and anthropogenic infrastructure) on soil redistribution processes along toposequences. Additionally, assessment of the importance of natural features for trapping and storing eroded soil, as promoted by the new Common Agricultural Policy (CAP) is a key requirement for both the sustainable management of the soil resource and the protection of downstream aquatic ecosystems from degradation resulting from increased sediment loads. Finally, the development of a perceptual model of soil movement aims to elucidate how linear landscape elements contribute to patterns of soil redistribution along cultivated and uncultivated toposequences.

2 Material and methods

2.1 Study area

The study was conducted along two representative toposequences located in the Spanish central Pre-Pyrenees (NE Spain), close to the northern boundary of the Ebro river basin (Figure 1). This area includes a freshwater lake. Estaña Lake, in the lower part of the landscape that has been under regional protection since 1997 and is included in the European NATURA 2000 network as a Site of Community Importance. The average annual precipitation is 595 mm (1997-2006) with two wet periods, spring and autumn, and a dry summer with high intensity rainfall events extending from July to October. The average annual temperature is 12.2º C, with thermal inversions common during the winter (López-Vicente et al., 2008). The Mediterranean agroecosystem of the study area comprises an intricate landscape, characterized by abrupt relief with slope gradients up to 34 %. The cultivated and uncultivated areas are heterogeneously distributed. The cultivated fields are located in the lower and mid slope areas and are separated by vegetation strips, while uncultivated areas predominate on the steep slopes. Winter barley is the main crop and, as indicated above, uncultivated areas include areas of Mediterranean forest, scrubland and abandoned fields recolonised by natural vegetation.

The predominant soil types along the toposequences are stony Calcisols and Regosols. Leptosols are restricted to the upper part of the slope under Mediterranean forest underlain by Muschelkalk facies, and Gypsisols cultivated for cereals are restricted to the lower part of one of the transects underlain by Keuper facies.

Two representative hillslope transects, extending from the divide to the lake, were selected to represent different toposequences within this agroecosystem (Figure 1). A total of 34 sampling sites, approximately 50 m apart were established along both transects. However, it was recognised that tillage erosion in fields delimited by furrows and tracks can cause significant soil redistribution both at the head and the bottom of the fields (Gaspar, 2011), and thus the spacing of the sampling sites on the lower cultivated part of the ST was reduced to 25 m, in order to provide a reliable representation of soil redistribution in this area (Figure 1).

The northern transect NT (S-N) is 300 m long and characterized by a 10 % slope. Its altitude ranges from 711 to 682 m and the seven sampling sites are located on a gentle north facing slope occupied exclusively by uncultivated areas. Regosols are restricted to the upper part of the transect while Calcisols predominated in the rest of the transect.

The southern transect ST (N-S) is 1110 m long and extends down a steeper south facing slope (21 % slope) with an altitude ranges from 894 to 676 m. The transect crosses patches of different land use. The uncultivated areas are located primarily on the upper and midslope sections of the transect on Calcisols and Regosols, whereas the cultivated fields are located on the midslope on stony Calcisols and Regosols and on the bottom slope on Gypsisols with a low stone content. Leptosols are found within the upper part of the transect under Mediterranean forest and on a thick Muschelkalk outcrop on the midslope. ST includes 27 sampling sites and is characterized by a rugged topography and the presence of agricultural terraces, a thick Muschelkalk outcrop on the midslope and vegetation strips, which have an important effect on hydrological processes as they reduce the local slope gradient, intercept runoff and trap eroded sediment.

Nine bulk cores were collected from sampling points located on cultivated soils and 24 sectioned profiles were collected from the sampling points on uncultivated soils, which were also the subject of another study investigating the depth distribution of unsupported ^{210}Pb (Gaspar, 2011). Sampling site ST-14 is located on a thick Muschelkalk outcrop and soil samples for $^{210}Pb_{ex}$ measurements were not collected from this point. The bulk cores obtained from the cultivated areas were collected using a 8.0 cm diameter hand-operated core sampler. The core depth always exceeded the plough depth (ca. 20 cm), with a maximum of 55 cm. The sectioned profiles were collected using a 10 x 10 cm steel box corer (Navas et al., 2008) at 2 cm depth intervals to a maximum depth of 10 - 14 cm depth, which had been shown by previous work in the study area to include the complete $^{210}Pb_{ex}$ profile in uncultivated soil (Gaspar, 2011). At each uncultivated sampling site, a three-sided frame was driven into the ground with the open end of the sampling frame facing downslope. The soil downslope of the sampler was carefully removed until a block of soil was enclosed within the sample frame. A blade was inserted into a series of grooves spaced at 2 cm on the sides of the device to section the profiles.

The samples collected from each sampling point along the transects were dried, gently disaggregated and sieved to < 2mm. The stone content (%) was determined as the proportion > 2mm. The < 2mm fraction was analysed to obtain the total $^{210}Pb_{ex}$ inventory (Bq m^{-2}), the soil organic carbon (SOC) content, and the mean clay, silt and sand content. The SOC content was determined by the dry combustion method using a LECO RC-612 multiphase carbon analyzer. In this case, a sub-sample of the < 2 mm fraction is inserted into a quartz tube, heated to 550 ºC and the SOC is oxidized to CO_2, which is selectively detected by an infrared (IR) gas analyser. Grain size analysis of the < 2mm fraction to determine the sand, silt and clay content (%) was undertaken using a laser granulometer. Prior to grain size analysis, organic matter was removed from the samples using 10% H_2O_2 heated to 80 °C and the mineral sediment was ultrasonically dispersed.

2.2 Using $^{210}Pb_{ex}$ as a sediment tracer

To determine the $^{210}Pb_{ex}$ inventory at each sampling point, a representative aliquot of the < 2mm fraction of the bulk core or the individual sections of the sectioned cores was placed into a cylindrical plastic container and sealed for 40 days prior to assay in order to achieve equilibrium between ^{226}Ra and its daughter ^{214}Pb. The $^{210}Pb_{ex}$ activity in the sample was measured by gamma-ray spectrometry, using a high resolution low energy coaxial HPGe detector coupled to an amplifier (broad energy detector (BeGe)). The detector had an efficiency of 30 % and a resolution of 1.9 keV, and was contained within a lead shield to reduce the background. Calibration was achieved using standard certified samples with the same geometry and bulk density as the measured samples. Count time was typically ca. 86,400 s, providing results with an analytical precision of ca. 10 - 15 % at the 95 % level of confidence. The total ^{210}Pb activity in the samples was measured at 46.5 keV, and the ^{226}Ra activity was obtained by measuring the activity of ^{214}Pb, a short-lived daughter of ^{226}Ra at 351.9 keV. The detection limits in Bq kg^{-1} for ^{210}Pb and ^{214}Pb were 7.45 and 1.26 Bq kg^{-1}, respectively. The $^{210}Pb_{ex}$ activity was determined by subtracting the ^{226}Ra activity from the total ^{210}Pb activity. The $^{210}Pb_{ex}$ inventories for individual sampling points were calculated using the measured $^{210}Pb_{ex}$ activities. With the sectioned cores this involved summing the values for the individual sections.

Estimates of soil redistribution rates are derived from $^{210}Pb_{ex}$ measurements by comparing the total inventory for an individual sampling soil with the local reference inventory for the study area and using a conversion model to estimate the erosion rate represented by a reduced inventory or the deposition rate represented by an increased inventory. In order to establish the $^{210}Pb_{ex}$ reference inventory, two sectioned profiles and seven bulk cores were collected from an undisturbed location adjacent to the sampled transects, with minimal slope and no evidence of erosion or deposition, such that no sediment redistribution was likely to have occurred over the past 100 years. The undisturbed nature of the reference sites was confirmed by the $^{210}Pb_{ex}$ depth profiles that provided a well-defined exponential depth distribution. Estimates of soil redistribution rates along the two transects investigated were obtained using the conversions models for cultivated and uncultivated soils described by Walling and He (1999a) and Walling et al. (2011).

Soil redistribution rates on cultivated soils were estimated using a mass balance model (mass balance model 2) developed at the University of Exeter (see Walling and He, 1999a). The model takes into account the continuous atmospheric deposition of $^{210}Pb_{ex}$ and its subsequent decay and its redistribution in association with soil erosion and deposition. In addition, the model considers the effect of particle size selectivity of sediment mobilization, and the transport and the removal of freshly deposited fallout $^{210}Pb_{ex}$ by erosion, before its incorporation into the tillage horizon. The basic form to estimate the erosion rate R (kg m^{-2} year^{-1}) can be expressed as Equation 1:

$$\frac{dA(t)}{dt} = (1-\Gamma)I(t) - \left(\lambda + P\frac{R}{d}\right)A(t) \qquad (1)$$

where $A(t)$ is the cumulative $^{210}Pb_{ex}$ inventory (Bq m^{-2}); d the tillage depth (kg m-2); λ is the ^{210}Pb decay constant (year^{-1}); $I(t)$ the annual fallout $^{210}Pb_{ex}$ deposition flux at time t (Bq m^{-2} year^{-1}); Γ the proportion of the freshly deposited $^{210}Pb_{ex}$

fallout input removed by water erosion before incorporation into the tillage layer; and P the particle size correction factor to take account of differences between the grain size composition of the mobilised sediment and the original soil (Walling ad He, 199a; Walling et al., 2003). The model used to estimate the deposition rate R' (kg m^{-2} $year^{-1}$) takes the form indicated by Equation 2:

$$A_{c,ex} = \int_{t_0}^{t} R' C_d(t') e^{e-\lambda(t-t')} dt' \qquad (2)$$

where $A_{c,ex}$ is the $^{210}Pb_{ex}$ inventory (Bq m^{-2}) and $C_d(t')$ represents the concentration of $^{210}Pb_{ex}$ in deposited sediment (Bq kg^{-1}). $C_d(t')$ can be estimated as the weighted mean $^{210}Pb_{ex}$ activity of the sediment eroded from the upslope contributing area.

A modified version of the diffusion and migration conversion model developed for ^{137}Cs measurements (Walling and He, 1999b) was used to estimate soil redistribution rates from $^{210}Pb_{ex}$ inventories at the uncultivated sampling points. This model assumes a constant fallout of $^{210}Pb_{ex}$ and takes into account post-depositional redistribution processes and their influence on the $^{210}Pb_{ex}$ depth distribution (Walling et al., 2011).

A diffusion coefficient D (kg^2 m^{-4} $year^{-1}$) is used to represent the net effect of the slow vertical redistribution of $^{210}Pb_{ex}$ by physicochemical and biological processes. The rate of soil loss R (kg m^{-2} $year^{-1}$) can be estimated from the reduction of the $^{210}Pb_{ex}$ inventory at the sampling point, relative to the reference inventory for the study site ($A_{u,ls}(t)$) and a model-derived estimate of the $^{210}Pb_{ex}$ content of the surface soil ($C_u(t')$), as indicated by Equation 3:

$$\int_{0}^{t} PRC_u(t') e^{-\lambda(t-t')} dt' = A_{u,ls}(t) \qquad (3)$$

The deposition rates R' (kg m^{-2} $year^{-1}$) can be estimated (Equation 4) from the increase in the $^{210}Pb_{ex}$ inventory compared with the local reference value ($A_{u,ex}(t)$), and the $^{210}Pb_{ex}$ content of deposited sediment soil ($C_d(t')$) (Walling et al., 2011).

$$R' = \frac{A_{u,ex}}{\int_0^t C_d(t')e^{-\lambda(t-t')}dt'} \quad (4)$$

$C_d(t')$ can be estimated as the weighted mean $^{210}Pb_{ex}$ activity of the sediment eroded from the upslope contributing area.

When applying the models to the $^{210}Pb_{ex}$ measurements obtained from the two transects, values of 4 kg m^{-2} and 1.0 were assumed for the relaxation depth (H) and particle size correction (P) parameters, respectively, in both models and a value of 1.0 was assumed for the proportion parameter (γ) in the mass balance model.

Once estimates of the soil redistribution rate were derived for each of the sampling points, the methodology proposed by Collins et al., (2001) was applied to each toposequence (NT and ST) to estimate the net soil redistribution rate associated with the two transects. In addition, in order to refine and adapt this technique for application to intricate Mediterranean landscapes, it is important to take account of the effects of linear landscape elements. The presence of agricultural terraces, buffer strips, rock outcrops and tracks can have an important effect on downslope runoff and sediment transfer as they reduce the slope gradient and length, and trap the eroded soil, influencing the distribution of areas of erosion and deposition along the slope.

Statistical analysis was performed by one-way analysis of variance (ANOVA), and the means were subjected to a least-significant difference test (F test) to indicate the main differences in $^{210}Pb_{ex}$ inventories and soil properties between cultivated and uncultivated sites, and the differences in the soil redistribution rates estimated from the $^{210}Pb_{ex}$ measurements between the different land uses, soil types and slope gradient.

3 Results and discussion

3.1 Assessment of soil redistribution rates using $^{210}Pb_{ex}$ inventories

The reference $^{210}Pb_{ex}$ inventory for the study area estimated from nine sampling points located on undisturbed soil with minimal slope adjacent to the study transects is 2019.8 ± 215.8 Bq m^{-2}. Figure 2 shows the depth distributions of $^{210}Pb_{ex}$ for a representative reference soil profile in the study area. This reference inventory is very similar to that reported for the area from a preliminary study reported by Gaspar et al. (2013) and is within the range of $^{210}Pb_{ex}$ reference inventories reported by Sanchez-Cabeza et al. (2007) for different parts of northern Spain (between 1044 and 8204 Bq m^{-2}, depending on the mean annual rainfall of the study site). However, the reference inventory obtained for the study area is smaller than values reported by other authors for different areas of the world, for example: 5170 Bq m^{-2} in the UK (Walling and He, 1999a), 5730 and 12860 Bq m^{-2} in China (Zhang, et al., 2003 and Zhang, et al., 2006, respectively), 6310 Bq m^{-2} (Kato et al., 2010) and 19703 Bq m^{-2} (Wakiyama et al., 2010) in Japan, 5266 (Porto et al., 2006), 14572 Bq m^{-2} (Porto et al., 2009) and 7598 Bq m^{-2} (Porto and Walling, 2012) in Italy, 34000 in Taiwan (Huh and Su, 2004), and between 3580 and 10060 Bq m^{-2} for different floodplain sites in England and Wales (Du and Walling, 2012).

The $^{210}Pb_{ex}$ inventories recorded along the two study transects showed significant variability, reaching a maximum of 7298.2 Bq m^{-2} (Table 1). The ANOVA test indicated that the $^{210}Pb_{ex}$ inventories were higher for cultivated soils than for uncultivated soils, although the differences were not statistically significant. A similar pattern has been previously documented in the study area for ^{137}Cs, and this trend confirms the importance of land use in controlling fallout radionuclide inventories and thus soil redistribution rates in the local area (Navas et al., 2012a; Gaspar et al., 2013).

The main soil properties analyzed showed values consistent with the characteristics of Mediterranean agroecosystems. Information on stone content, SOC content and grain size composition for cultivated and uncultivated soils are presented in Table 1. The SOC and stone content were significantly higher in uncultivated soils. In cultivated soils the maximum values of SOC did not exceed 2.3 %, confirming the impact of long-term and intense agricultural use on SOC content (Navas et al., 2011). The relative magnitude of the clay, silt and sand fractions varied greatly between the sampling points. However, no significant difference was found between the two land uses, with silt-loam being the predominant texture.

After isolating the land use factor, only SOC showed significant differences between different soil types. For cultivated soils, higher inventories of $^{210}Pb_{ex}$ were found on Gypsisols, while Calcisols showed significantly higher mean values of SOC and slightly higher mean values of stone and sand content. In uncultivated areas, significantly higher mean values of SOC was found on Leptosols, which in turn have slightly higher values of $^{210}Pb_{ex}$ inventory and stone content (Table 2).

For the northern transect (NT), the lack of significant reduction or increase in inventory values for the sampling points indicates that these points have not experienced significant soil redistribution over the past 100 years, and particularly in recent years. In contrast, significant increases and reductions in inventory values, relative to the reference inventory, for the sampling points on the southern transect (ST), particularly for cultivated points, suggest that these points have experienced appreciable soil loss or deposition over that period, and indicate that significant soil redistribution has occurred along transect ST, in marked contrast with the NT transect.

The soil redistribution rates (Mg ha^{-1} year^{-1}), derived from the $^{210}Pb_{ex}$ inventories using the models described above and shown in Figure 3, indicate that erosion rates range between 0.1 and 83.7 Mg ha^{-1} year^{-1} and sedimentation rates range between 0.08 and 74.8 Mg ha^{-1} year^{-1}. The highest values were found on cultivated soils, whereas on uncultivated soils, erosion and deposition rates did not exceed 2.4 and 5.6 Mg ha^{-1} year^{-1}, respectively (Table 3). As shown in Figure 3, the soil redistribution rates follow quite closely the changes in land use. For the uncultivated transect (NT) most sampling points recorded low erosion rates, with a maximum of 2.4 Mg ha^{-1} year^{-1} (NT-6) and most values close to stability (NT-1, NT-4, NT-5). The highest sedimentation rates were found at the bottom part of the transect (NT-7) and did not exceed 5.6 Mg ha^{-1} year^{-1}. On the contrary, the combined effects of topography and tillage have caused different patterns of soil redistribution along the ST. Uncultivated areas on ST evidence similar soil redistribution rates to those found on NT and soil stability predominates. In the upper part of ST the dense forest protected the soil surface from erosion (ST-1, ST-3) and higher deposition rates, that did not exceed 1.3 Mg ha^{-1} year^{-1} (ST-20), were identified on the relatively flat areas (ST-6, ST-10, ST-17). The highest erosion rate within the uncultivated areas was located at ST-19 (2.3 Mg ha^{-1} year^{-1}), which corresponds to open scrubland. On the steeper cultivated slopes, sampling points ST-13, ST-15 and ST-16 recorded high erosion rates (between 5.4 and 54.20 Mg ha^{-1} year^{-1}). In contrast, on cultivated flat areas at the bottom part of the ST, sampling points ST-23, ST-24, ST-26 and ST-27 evidenced the highest deposition rates, but the highest erosion rate was also found at ST-25 (83.7 Mg ha^{-1} year^{-1}). Previous research in this area with ^{137}Cs and ^{210}Pb$_{ex}$ (Gaspar et al., 2013) provide evidence that tillage erosion was important in these cultivated fields. The soil redistribution rates estimated from the ^{210}Pb$_{ex}$ measurements are in agreement with those obtained from ^{137}Cs measurements in the same study area, using appropriate conversion models (Soto and Navas, 2004, 2008), which ranged between 2.6 and 31.9 Mg ha^{-1} year^{-1} for erosion rates, and between 0.2 and 24.5 Mg ha^{-1} year^{-1} for deposition rates. These results demonstrate the important effect of agricultural activities on soil redistribution. The presence of ridges and furrows causes a local increase in slope gradient on the side of the furrow, relative to the natural slope, which will increase rates of interrill erosion (Junge et al., 2010).

The mean erosion rates for the cultivated fields were significantly higher than for the uncultivated areas. Slightly higher erosion rates were found on Regosols than on Leptosols and Calcisols, although differences were not significant, while on Gypsisols the mean erosion rates were significantly higher. Table 4 indicates that erosion rates were similar in areas with average slope between 0 to 12 % and 12 to 24 % and that these rates appeared to be higher than those on steeper slopes (> 24 %), although the difference was not statistically significant. The mean deposition rates were significantly higher for cultivated areas and on Gypsisols. However, unlike the erosion rates, significantly higher deposition rates were found on flat areas (0 to 12 %) (Table 4).

In the study area, land use, soil type and slope gradient are linked. Most of the uncultivated profiles were on Leptosols and Calcisols, located along the upper part of ST and along NT and these points had the lowest rates of soil redistribution. While, most cultivated sampling points were on Gypsisols, these were located on the flatter lower part of ST, which recorded the highest redistribution rates (both erosion and deposition). On Regosols, the cultivated sampling points were on steep slopes, while the sampling points on uncultivated areas consisted of open scrubland. Both favoured redistribution processes.

Principal components loadings and biplot after varimax rotation (Table 5, Figure 4) show that for erosion rates, three components were retained with eigenvalues higher than one, explaining 74 % of total variance. The first principal component, which represents 32 % of the total of variance, showed high values for the variables related to grain size. The second component, with 29 % of total variance, showed high loading values of the parameters related to land use and erosion rates, which were negatively correlated with SOC and also with stone content but the estimated communality of this particular variable is lower than 0.5 and represents a low proportion of the variance. The third component was associated with the slope factor, which was negatively correlated with SOC, and represents 13 % of variance (Table 5.a). For deposition rates, two components explained 78 % of the total variance. The first component, which represents 54 % of the total variance, showed high loading values for the parameters related to land use and deposition rates, which were negatively correlated with SOC, slope factor and stoniness, while the second component, with 24 % of total variance, showed high loading values of the parameters related to grain size (Table 5.b).

Although PCA cannot be used numerically for prediction purposes, the PCA biplot (Figure 4a, 4b) is of interest as it indicates the level of correlation between the analyzed variables. Both erosion and deposition rates are positively correlated with land use. Likewise, the fact that SOC is negatively correlated with erosion rates can be interpreted to mean that soil loss is associated with loss of organic carbon (Figure 4.a), as reported for similar environments by Navas et al. (2012b) and in agreement with Ritchie and McCarty (2008), who also reported strong links between soil redistribution and soil organic carbon concentrations in agricultural soils. In addition, the fact that stone content and slope are negatively correlated with deposition rates can be interpreted to mean that in flat areas evidencing a lower stone content deposition processes predominate (Figure 4.b).

Despite the small sample size (n=20 for erosion rates and n=13 for deposition rates), the communality of most variables was higher than 0.5 (Table 5a, 5b), thus the extracted components account for a substantial proportion of the variable’s variance. This means that these variables are reflected well via the extracted components, and hence that the PCA analysis was reliable.

3.2 A quantitative perceptual model for estimating soil redistribution rates and the effect of linear landscape elements

Assuming that each transect represents a 1 m wide strip, values of soil redistribution rate obtained for each sampling point were used to calculate equivalent values of soil loss or deposition (kg year^{-1}) for individual slope segments, extending halfway to the adjacent coring points from the sampling point in each direction, as reported by Collins et al. (2001), Walling et al. (2003) and Estrany et al. (2010). However, this methodology was modified to adapt it to the characteristics of the study transects, in order to take into account changes in land use and the presence of linear landscape elements. This was achieved by relating the segment length to vegetation cover and introducing the linear landscape elements.

The resulting values for each segment were summed to provide a total erosion and total deposition, respectively, thus obtaining net soil loss for each transect (Mg ha^{-1} year^{-1}) and the sediment delivery ratio (%) (cf. Walling et al., 2003). For NT, the total erosion is estimated at 26 kg year^{-1} and total deposition at 25.8 kg year^{-1}. The net soil loss of 0.2 kg year^{-1} (0.01 Mg ha^{-1} year^{-1} and a sediment delivery ratio of 0.7 %) indicates that soil redistribution processes have a limited effect on this transect. The presence of a stone embankment between NT-4 and NT-5, and an unpaved trail between NT-6 and NT-7 is likely to modify the runoff and sediment connectivity along the transect, except during intense rainfall events. In contrast, for ST the total erosion is estimated to be 637 kg year^{-1} and total deposition at 705 kg year^{-1}, representing a net soil accumulation of 68 kg year^{-1} (1.24 Mg ha^{-1} year^{-1} and a negative sediment delivery ratio), with this especially concentrated along the bottom part of the ST.

Transect ST is characterized by the presence of a thick Muschelkalk outcrop at the midslope, between ST-13 and ST-15, which disrupts the runoff and sediment connectivity along the transect. In addition, an unpaved trail located on the bottom slope (between ST-24 and ST-25), a system of old terraces located in the upper part of the transect (between ST-10 and ST-11) and several vegetation strips (Figure 5), also modify the topography and change the runoff and sediment connectivity along the transect.

Considering the natural elements and human modifications, mentioned above, transect ST was divided into seven sections (Figure 5). During normal rainfall events the linear landscape elements restrict the runoff and the downslope transfer of soil previously eroded within each of the seven sections. However, during intense and erosive rainfall events only the thick outcrop disrupts the soil redistribution processes along ST. In the upper part of the transect, the vegetation cover on uncultivated areas is dense and, in spite of the presence of the steepest slopes, the first three sections recorded low values of net soil loss (0.3, 0.3, 2.8 Mg ha^{-1} $year^{-1}$, respectively, and sediment delivery ratios of 63, 100 and 100 %, respectively). In sections four and five higher values of net soil loss coincide with cultivated soils on steep slope (54.2 and 12.9 Mg ha^{-1} $year^{-1}$, respectively, and the corresponding sediment delivery ratios were 100 %). Section six is characterized by low erosion rates on uncultivated areas and net soil deposition (6.5 Mg ha^{-1} $year^{-1}$), which occurs in the cultivated fields above the trail. The last sections correspond with cultivated flat areas below the trail, with higher net soil deposition (1.91 Mg ha^{-1} $year^{-1}$).

This methodology provides information regarding erosion and deposition rates, as well as the net soil loss from the transects, and how land use and linear landscape elements modify the soil redistribution processes and sediment connectivity.

The patterns of $^{210}Pb_{ex}$ redistribution along both NT and ST demonstrate that in Mediterranean environments cultivated land exerts an important control on soil loss stressing the need to encourage the participation of the farmers in soil conservation programs. Furthermore, these results suggest that deposition rates associated with cultivated areas are affected by the presence of flat topography and soil conservation practices, while deposition rates on uncultivated areas are linked to changes from convex to concave slopes, the presence of transverse terraces and vegetation buffer strips, which reduce runoff velocity. These results emphasize the potential of the new green areas program proposed by CAP to control soil loss in agricultural ecosystems.

Sediment mobilised from the upslope areas may be deposited in the Estaña lake located downslope of the investigated transects. The net soil deposition rates obtained for NT and ST are influenced by the location of the soil sampling sites selected along 1 m wide strip. However, previous research using ^{137}Cs measurements (Gaspar et al., 2013) showed high activity of ^{137}Cs in deeper layers at a sampling point situated on the margin of the Estaña lake, adjacent to ST-27 at the bottom of the ST. This profile corresponds to a lake sediment deposit, as indicated by the presence of the 1963 ^{137}Cs peak at a depth of 45 cm, which means an accumulation sediment of 113 Mg ha^{-1} year^{-1} at this point.

4 Conclusions

This study has demonstrated the potential of $^{210}Pb_{ex}$ measurements to estimate soil erosion and deposition along the toposequences that are characteristic of hillslopes in mountain Mediterranean agroecosystems. For intricate transects, the sampling strategy should take into account changes in land use and the presence of linear elements in cultivated fields that might intensify tillage erosion at the head of the fields. For transects with homogeneous land use, a spacing of 50 m between sampling points is considered sufficient to provide meaningful estimates of soil redistribution rates. This contribution describes similar soil redistribution patterns along the toposequences to those established using ^{137}Cs, $^{210}Pb_{ex}$ and prediction models in previous research.

The spatial variability of soil redistribution rates along the toposequences was closely controlled by land use that was in turn closely related to vegetation cover, topography, soil type and slope gradient. Our results show that on steep cultivated slopes erosion processes predominated, whereas uncultivated areas were characterized by lower soil redistribution rates. On the flat areas at the bottom of both transects, sedimentation processes dominated over erosion. The marked variations of SOC content along the transect clearly reflect the variety of land use along the transects and their complex physiography.

Land use and slope gradient exert important controls on the soil redistribution rates. For steep slopes on the upper part of the transects, the open Mediterranean forest and scrubland protect the soil surface from erosion, while the cultivated soils are more vulnerable to erosion and soil redistribution is more intense. Vegetation cover together with topography and tillage are key factors affecting the pattern of soil redistribution on the transects.

Assessing erosion and deposition rates for cultivated and uncultivated soils has proved useful for understanding the dynamics of soil redistribution in mountain agroecosystems. The application of a quantitative perceptual model has provided information to assess the effects of linear landscape elements along complex toposequences. This research has contributed information on the potential role of linear landscape elements and vegetation buffer strips in controlling sediment transfer along hillslopes within Mediterranean agroecosystems.

Acknowledgements

Financial support from CICYT project EROMED (CGL2011-25486/BTE) is gratefully acknowledged. Financial support of the Spanish CAI social work bank for a postdoctoral fellowship during 2012 is gratefully acknowledged.

References

Benmansour, M., Mabit, L., Nouira, A., Moussadek, R., Bouksirate, H., Duchemin, M., Benkdad, A., 2013. Assessment of soil erosion and deposition rates in a Moroccan agricultural field using fallout ^{137}Cs and $^{210}Pb_{ex}$. J. Environ. Radioactiv. 115, 97-106.

Cerdà, A., 1997. Soil erosion after land abandonment in a semiarid environment of southeastern Spain. Arid. Soil Res. Rehabil. 11(2), 163-176.

Collins, A.L., Walling, D.E., Sichingabula, H.M., Leeks, G.J.L., 2001. Using ^{137}Cs measurements to quantify soil erosion and redistribution rates for areas under different land use in the Upper Kaleya River basin, southern Zambia. Geoderma 104, 299-323.

Du, P., Walling, D.E., 2011. Using ^{137}Cs measurements to investigate the influence of erosion and soil redistribution on soil properties. Appl. Radiat. Isot. 69, 717-726.

Estrany, J., García, C., Walling, D., 2010. An investigation of soil erosion and redistribution in a Mediterranean lowland agricultural catchment using caesium-137. Int. J. Sediment Res. 25, 1-16.

García-Ruiz, J.M., 2010. The effects of land uses on soil erosion in Spain: A review. Catena 81, 1-11.

García-Ruiz, J.M., Regües, D., Alvera, B., Lana-Renault, N., Serrano-Muela, P., Nadal-Romero, E., Navas, A., Latron, J., Martí-Bono, C., Arnáez, J., 2008. Flood generation and sediment transport in experimental catchments affected by land use changes in the central Pyrenees. J. Hydrol. 356 (1-2), 245-260.

Gaspar, L., 2011. Evaluación de la movilización y pérdida de suelo en agrosistemas de secano mediante los radiotrazadores ^{137}Cs y ^{210}Pb$_{ex}$. PhD Thesis, University of Zaragoza. Spain, pp. 455.

Gaspar, L., Navas, A., Walling, D.E., Machín, J. y Gómez Arozamena, J., 2013. Using ^{137}Cs and ^{210}Pb to assess soil redistribution on slopes at different temporal scales. Catena 102, 46-54.

He, Q., Walling, D.E., 1996. Interpreting particle size effects in the absorption of ^{137}Cs and unsupported ^{210}Pb by mineral soils and sediments. J. Environ. Radioactiv. 30, 117-137.

Huh, C.-A., Su, C.-C., 2004. Distribution of fallout radionuclides (^{7}Be, ^{137}Cs, ^{210}Pb and $^{239, 240}$Pu) in soils of Taiwan. J. Environ. Radioactiv. 77 (1), 87-100.

Junge, B., Mabit, L., Dercon, G., Walling, D.E. Abaidoo, R., Chikoye, D., Stahr, K., 2010. First use of the ^{137}Cs technique in Nigeria for estimating medium-term soil redistribution rates on cultivated farmland. Soil Till. Res. 110, 211-220.

Kato, H., Onda, Y., Tanaka, Y., 2010. Using ^{137}Cs and ^{210}Pb$_{ex}$ measurements to estimate soil redistribution rates on semi-arid grassland in Mongolia. Geomorphology 114, 508-519.

López-Vicente, M., Navas, A., 2010. Relating soil erosion and sediment yield to geomorphic features and erosion processes at the catchment scale in the Spanish Pre-Pyrenees. Environ. Earth Sci. 61, 143-158.

López-Vicente, M., Navas, A., Machín, J., 2008. Identifying erosive periods by using RUSLE factors in mountain fields of the Central Spanish Pyrenees. Hydrol. Earth Syst. Sc. 12 (2), 523-535.

Navas, A., Gaspar, L., Quijano, L., López-Vicente, M., Machín, J., 2012b. Patterns of soil organic carbon and nitrogen in relation to soil movement under different land uses in mountain fields (South Central Pyrenees). Catena 94, 43-52.

Navas, A., López-Vicente, M., Gaspar, L. y Machín, J. 2012a. Assessing soil redistribution in a complex karst catchment using fallout ^{137}Cs and GIS. Geomorphology doi:10.1016/j.geomorph.2012.03.018.

Navas, A., Valero-Garcés, B., Gaspar, L., Palazón, L., 2011. Radionuclides and stable elements in the sediments of the Yesa Reservoir, Central Spanish Pyrenees. J. Soils Sediment. 11, 1082-1098.

Navas, A., Walling, D.E., Gaspar, L., Machín, J., 2008. Use of Beryllium-7 to assess soil redistribution by erosion in two contrasting Mediterranean environments. In: Sediment Dynamics in Changing Environments. Schmidt, J., Cochrane, T., Phillips, C., Elliott, S., Davies, T., Basher, L. (Eds.) IAHS Publi. 325, pp. 43-51.

Porto, P., Walling, D.E., 2012. Validating the use of ^{137}Cs and $^{210}Pb_{ex}$ measurements to estimate rates of soil loss from cultivated land in southern Italy. J. Environ. Radioact. 106, 47-57.

Porto, P., Walling, D.E., Callegari, G., Capra, A., 2009. Using caesium-137 and unsupported lead-210 measurements to explore the relationship between sediment mobilisation, sediment delivery and sediment yield for a Calabrian catchment. Mar. and Freshwater Res. 60, 680-689.

Porto, P., Walling, D.E., Callegari, G., Catona, F., 2006. Using fallout lead-210 measurements to estimate soil erosion in three small catchments in southern Italy. Water Air Soil Pollut. 6, 657-667.

Ritchie, J.C., McCarty, G.W., 2003. ^{137}Cesium and soil carbon in a small agricultural watershed. Soil Till. Res. 69, 45-51.

Ritchie, J.C., McCarty. G.W., 2008. Redistribution of soil and soil organic carbon on agricultural landscapes. In: Sediment Dynamics in Changing Environments. Schmidt, J., Cochrane, T., Phillips, C., Elliott, S., Davies, T., Basher, L. (Eds.) IAHS Publi. 325, pp. 135-138.

Sánchez-Cabeza, J.A., Garcia-Talavera, M., Costa, E., Peña, V., Garcia-Orellana, J., Nalda, C., 2007. Regional calibration of erosion radiotracers (^{210}Pb and ^{137}Cs): Atmospheric fluxes to soils (N Spain). Environ. Sci. Technol. 41(4), 1324-1330.

Soto, J., Navas, A., 2004. A model of ^{137}Cs activity profile for soil erosion studies in uncultivated soils of Mediterranean environments. J. Arid Environ. 59, 719-730.

Soto, J., Navas, A., 2008. A simple model of Cs-137 profile to estimate soil redistribution in cultivated stony soils. Radiat. Meas. 43, 1285-1293.

Wakiyama, Y., Onda, Y., Mizugaki, S., Asai, H., Hiramatsu, S., 2010. Soil erosion rates on forested mountain hillslopes estimated using ^{137}Cs and ^{210}Pb$_{ex}$. Geoderma 159, 39-52.

Wallbrink, P.J., Murray, A.S., 1993. The use of fallout radionuclide as indicators of erosion processes. Hydrol. Process. 7, 297-304.

Walling, D.E., Collins, A.L., Sichingabula, H.M., 2003. Using unsupported lead-210 measurements to investigate soil erosion and sediment delivery in a small Zambian catchment. Geomorphology 52, 193-213.

Walling, D.E., He, Q., 1999a. Using fallout lead-210 measurements to estimate soil erosion on cultivated land. Soil Sci. Soc. Am. J. 63, 1404-1412.

Walling, D. E., He, Q., 1999b. Improved models for estimating soil erosion rates from Cesium-137 measurements. J. Environ. Qual., 28, 611-622.

Walling, D.E., Quine, T.A., 1995. The use of fallout radionuclide in soil erosion investigations. In: Nuclear Techniques in Soil-Plant Studies for Sustainable Agriculture and Environmental Preservation. International Atomic Energy Agency Publication ST1/PUB/947, 597-619.

Walling, D.E., Zhang, Y., He, Q., 2011. Models for deriving estimates of erosion and deposition rates from fallout radionuclide (caesium-137, excess lead-210 and beryllium-7) measurements and the development of user-friendly software for model implementation. In: Impact of Soil Conservation Measures on Erosion Control and Soil Quality. International Atomic Energy Agency Publication IAEA-TECDOC-1665, 11-33.

Zhang, X., Qi, Y., Walling, D.E., He, X., Wen, A., Fu, J., 2006. A preliminary assessment of the potential for using $^{210}Pb_{ex}$ measurement to estimate soil redistribution rates on cultivated slopes in the Sichuan Hilly Basin of China. Catena 68, 1-9.

Zhang, X., Walling, D.E., Feng, M., Wen, A., 2003. $^{210}Pb_{ex}$ depth distribution in soil and calibration models for assessment of soil erosion rates from $^{210}Pb_{ex}$ measurements. Chinese Sci. Bulletin 48 (8), 813-818

Tables

Table 1. Basic statistics of $^{210}Pb_{ex}$ inventories (Bq m^{-2}), and the main physicochemical soil properties for cultivated and uncultivated soils. Different letters indicate significant differences at the p-level < 0.05 between cultivated and uncultivated soils.

	Cultivated n=9					Uncultivated n=24				
	Min.	Max.	Mean		SD	Min.	Max.	Mean		SD
$^{210}Pb_{ex}$ Bq m^{-2}	b.d.l.	7298.2	2975.9	a	2904.4	325.7	5729.4	1933.2	a	1042.4
SOC %	0.6	2.3	1.2	a	0.6	1.0	10.1	4.6	b	2.6
Stoniness %	5.0	55.9	27.0	a	16.6	20.6	70.4	45.3	b	12.6
Clay %	15.6	37.4	24.5	a	6.1	11.9	40.8	23.4	a	5.4
Silt %	35.7	77.6	63.5	a	13.4	41.9	78.6	63.8	a	8.6
Sand %	0.5	48.7	12.0	a	16.4	0.1	46.2	12.8	a	11.2

SD *standard deviation*
b.d.l. *below detection limit*

Table 2. Mean values of $^{210}Pb_{ex}$ inventories (Bq m^{-2}) and the main physicochemical soil properties for different soil types in cultivated and uncultivated soils.

		Cultivated			Uncultivated		
		Calcisols n=1	Regosols n=4	Gypsisols n=4	Leptosols n=3	Calcisols n=14	Regosols n=7
$^{210}Pb_{ex}$ Bq m^{-2}	Mean	1654.6	1406.1	4876.0	1809.5	2056.2	1740.4
	SD	-	1837.0	3230.8	286.6	1208.5	942.2
SOC %	Mean	2.3	1.1	0.8	8.0	3.9	4.4
	SD	-	0.5	0.2	1.8	1.8	3.2
Stoniness %	Mean	48.8	33.1	15.2	53.9	41.7	49.0
	SD	-	16.7	7.7	2.9	12.5	13.7
Clay %	Mean	21.3	21.3	28.5	23.9	24.2	21.8
	SD	-	5.1	6.0	2.7	6.6	3.4
Silt %	Mean	49.9	64.4	66.1	67.1	60.3	69.2
	SD	-	19.5	5.1	2.5	7.7	9.2
Sand %	Mean	28.8	14.3	5.4	9.1	15.5	9.0
	SD	-	22.9	5.3	5.0	12.0	10.7

SD *standard deviation*

Table 3. Summary statistics of soil erosion and deposition rates (Mg ha^{-1} year^{-1}) for sampling sites on cultivated and uncultivated soils.

Mg ha^{-1} year^{-1}	n	Median	Mean	SD	SE	Min.	Max.	CV %
Erosion								
Cultivated	5	12.9	32.1	35.4	15.8	4.2	83.7	110.3
Uncultivated	15	0.5	0.9	0.8	0.2	0.1	2.4	89.1
Deposition								
Cultivated	4	56.5	54.1	20.6	10.3	28.6	74.75	38.1
Uncultivated	9	0.5	1.1	1.8	0.6	0.1	5.6	162.2

SD *standard deviation*
SE *standard error*

Table 4. Multiple range test for soil erosion and deposition rates (Mg ha^{-1} $year^{-1}$) associated with different edaphic and physiographic characteristics. Different letters indicate significant differences at the p-level < 0.05 between different land uses, soil types and slope gradients, respectively.

	Erosion rate Mg ha^{-1} $year^{-1}$				Deposition rate Mg ha^{-1} $year^{-1}$			
	n	Mean		SD	n	Mean		SD
Land use								
Uncultivated	15	0.9	a	0.8	9	1.1	a	1.8
Cultivated	5	32.1	b	35.4	4	54.1	b	20.6
Soil type								
Leptosols	2	0.5	a	0.3	1	0.1	a	-
Calcisols	10	1.2	a	1.6	5	1.5	a	2.3
Regosols	7	10.9	a	19.6	4	7.7	a	13.9
Gypsisols	1	83.7	b		3	62.6	b	14.3
Slope %								
0-12	9	10.5	a	27..5	6	37.2	b	30.7
12-24	7	10.6	a	19.8	5	0.3	a	0.2
> 24	4	1.1	a	0.9	2	0.8	ab	0.8

SD *standard deviation*

Table 5.a. Varimax rotated principal component loading (PCi) for the three first components (erosion rates). Loading factors higher than 0.5 (absolute value) are shown in bold.

	PC1	PC2	PC3	Estimated communality
Use	0.31186	**0.83757**	0.02315	**0.79931**
Stoniness %	0.18808	**-0.63599**	0.18469	0.47397
Erosion rates Mg ha^{-1} $year^{-1}$	-0.05773	**0.86661**	-0.07046	**0.75931**
Clay %	**-0.75604**	0.07373	0.02519	**0.57767**
Silt %	**-0.83205**	-0.03449	-0.16506	**0.72074**
Sand %	**0.97829**	-0.00531	0.11993	**0.97147**
SOC %	0.11328	**-0.66614**	**-0.58696**	**0.80110**
Slope %	0.20854	-0.20802	**0.83489**	**0.78381**

Table 5.b. Varimax rotated principal component loading (PCi) for the two first components (deposition rates). Loading factors higher than 0.5 (absolute value) are shown in bold.

	PC1	PC2	Estimated communality
Use	**-0.91573**	0.28580	**0.92023**
Stoniness %	**0.81778**	-0.24505	**0.72882**
Deposition rates Mg ha^{-1} $year^{-1}$	**-0.92483**	0.18565	**0.88977**
Clay %	-0.37995	**0.59488**	0.49824
Silt %	0.06915	**0.91820**	**0.84788**
Sand %	0.12374	**-0.97653**	**0.96893**
SOC %	**0.61104**	**-0.61082**	**0.74646**
Slope %	**0.77786**	0.16928	**0.63373**

Figures

Figure 1. The study area located in the northern border of central part of the Ebro basin (NE Spain) and the 34 sampling sites situated along southern (ST) and northern (NT) transects.

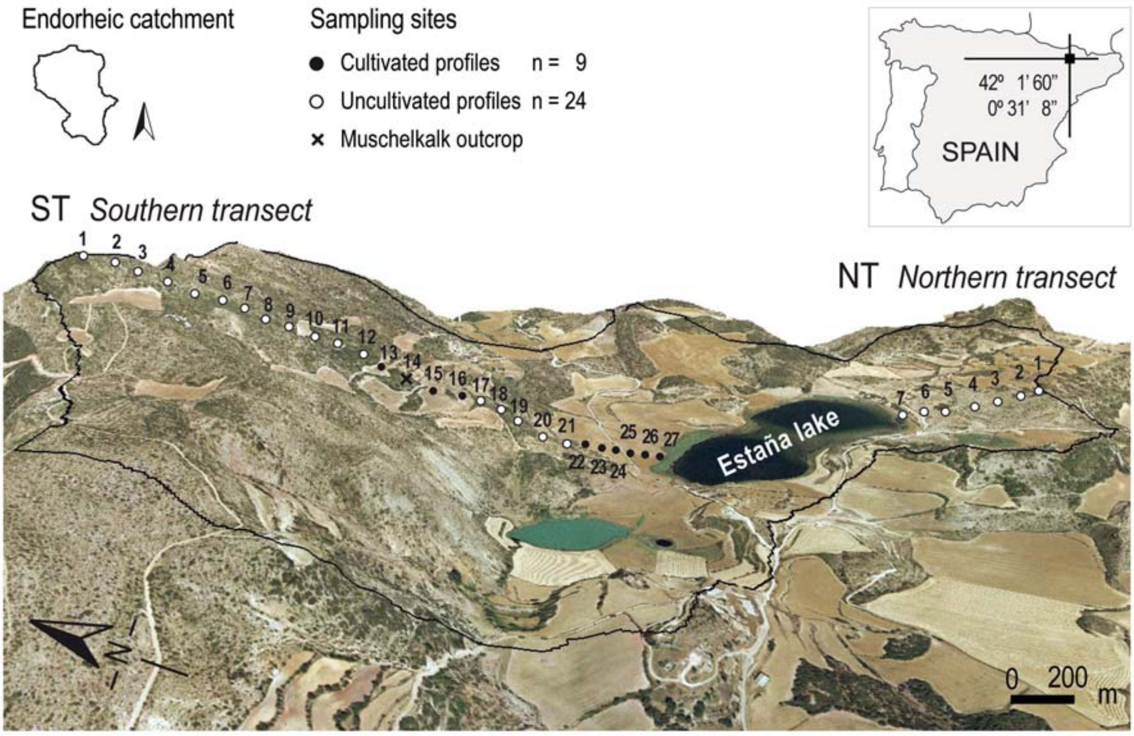

Figure 2. Representative depth distribution of $^{210}Pb_{ex}$ at the reference site.

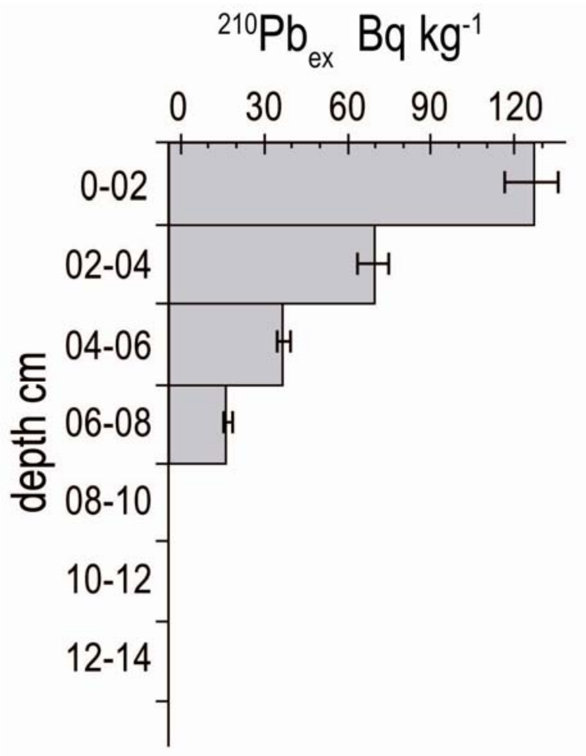

Figure 3. Estimates of soil redistribution rates based on the $^{210}Pb_{ex}$ inventory measurements for the individual sampling points along northern (NT) and southern (ST) transect. Black numbers indicate cultivated soil profiles and grey numbers indicate uncultivated soil profiles.

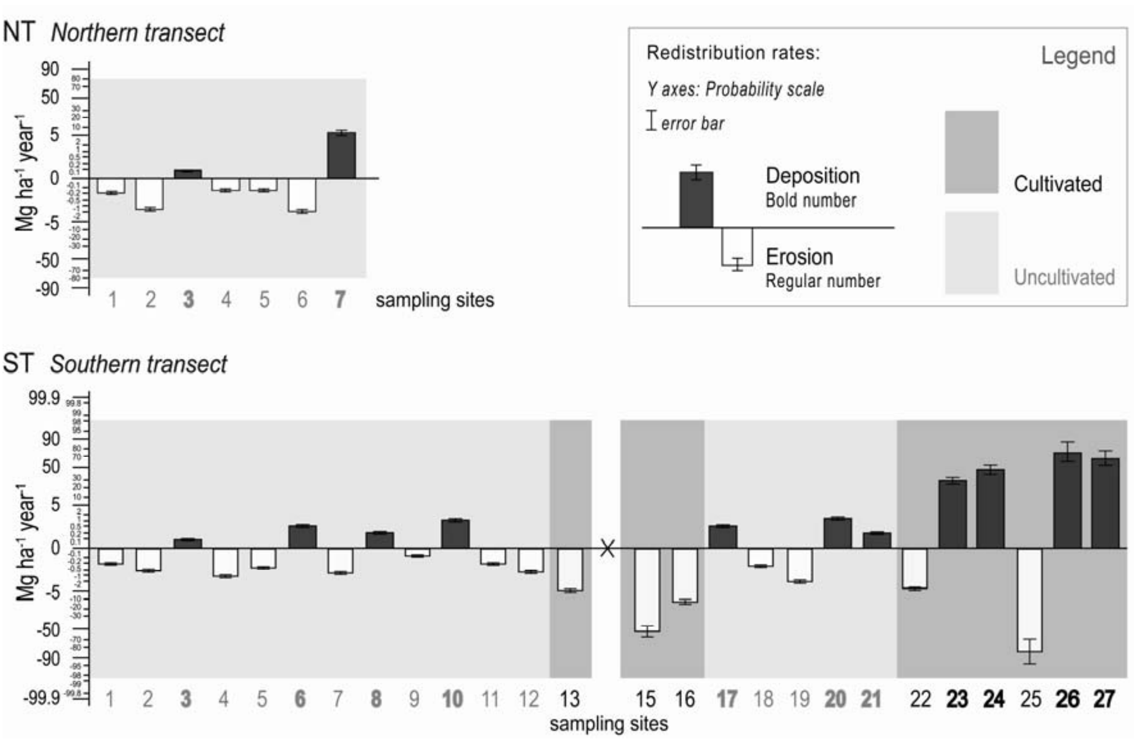

Figure 4. PCA biplot: dispersion diagram and principal components loadings, PC loading 1 vs. PC loading 2 of cultivated and uncultivated soil samples after PCA Varimax rotated for a) erosion rates and b) deposition rates.

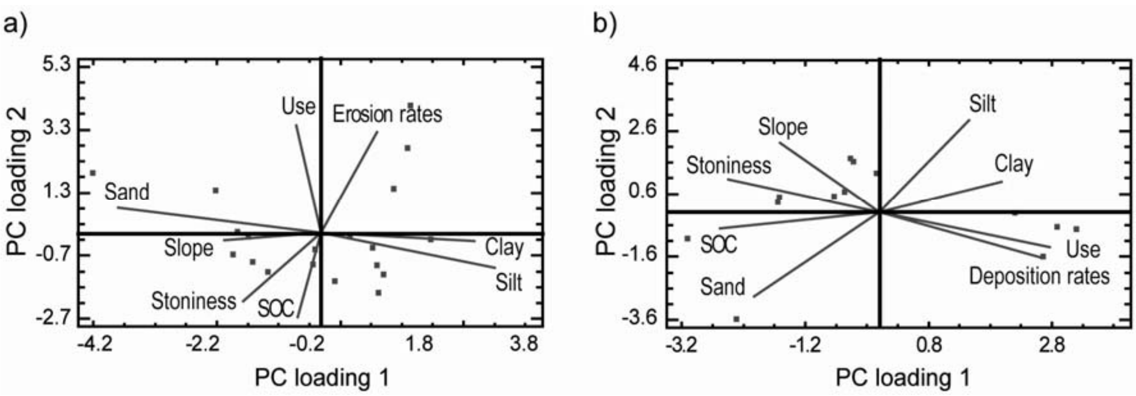

Figure 5. Estimates of soil redistribution rates for individual slope segments and net soil loss along the northern (NT) and southern (ST) transects.